

PAPER • OPEN ACCESS

Fully integrated numerical design tool to assess the thermal performance of phase change materials (PCM) in the built environment

To cite this article: D. Rubinetti *et al* 2020 *IOP Conf. Ser.: Earth Environ. Sci.* **410** 012114

View the [article online](#) for updates and enhancements.

Fully integrated numerical design tool to assess the thermal performance of phase change materials (PCM) in the built environment

D. Rubinetti¹, D. A. Weiss¹, D. Kraniotis² and A. Chaudhuri²

¹ Institute of Thermal and Fluid Engineering, University of Applied Sciences and Arts Northwestern Switzerland

² Department of Civil Engineering and Energy Technology, Oslo Metropolitan University, Norway

E-mail: donato.rubinetti@fhnw.ch

Abstract. Thermal energy storage with phase change materials (PCM) is a promising candidate to promote resource sustainability in buildings. The intelligent selection and usage of a PCM within the structure of a building poses a challenging engineering task due to the highly dynamic nature of occurring heat transfers. This work features a step-by-step FEM modeling guideline to assist the design of building structures by means of a 1D heat conduction scheme. The phase change functionality is based on the apparent heat capacity method and extended by ordinary differential equations to account for the thermal hysteresis of materials with different melting and freezing temperatures. The set of equations is solved alongside with logical expressions representing a thermostat functionality to assess the external energy demand. Two proof-of-concept examples for PCM usage in typical Swiss and Greek wall structures are given.

1. Introduction

Some materials exhibit an exceptionally large release and absorption of heat during the melting and freezing process. Such materials are labeled as phase change materials (PCM). Among the vast selection of commercially available PCMs certain types pose a promising attempt at improving the energy efficiency of buildings [1].

Experimental and numerical research related to PCM has received notable attention both on material and room level, respectively. Investigations on material level provide deep understanding of the melting behavior of PCM, the propagation of the phase change interface and optimization possibilities [2]. Such optimization possibilities may include the increase of the notoriously low thermal conductivity of PCM by *e.g.* addition of nanoparticles (nano-enhanced PCM). On room level, the overall performance of PCM in interaction with ambient thermal properties is investigated. Numerical work on room level proves *a priori* delicate due to the large computational resources required. Experimental work on room level, on the other hand, comes with elevated research costs [3].

The work described in this contribution aims at combining the essentials of material- and room-level PCM analysis to create a fully integrated numerical design tool.



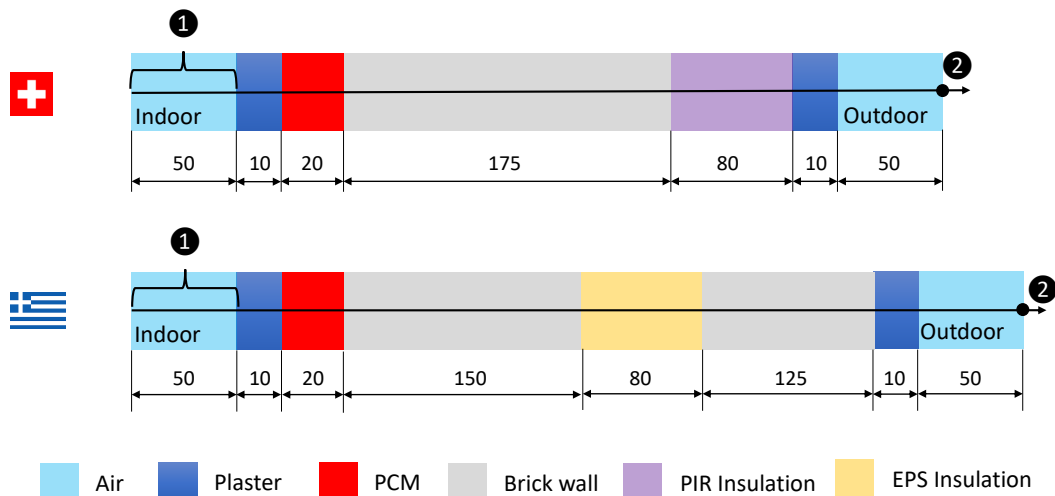


Figure 1. Geometrical arrangement of the examined wall crosssections according to typical Swiss and Greek regulatories. Thicknesses expressed in millimeters.

2. Physical Model

2.1. Geometry

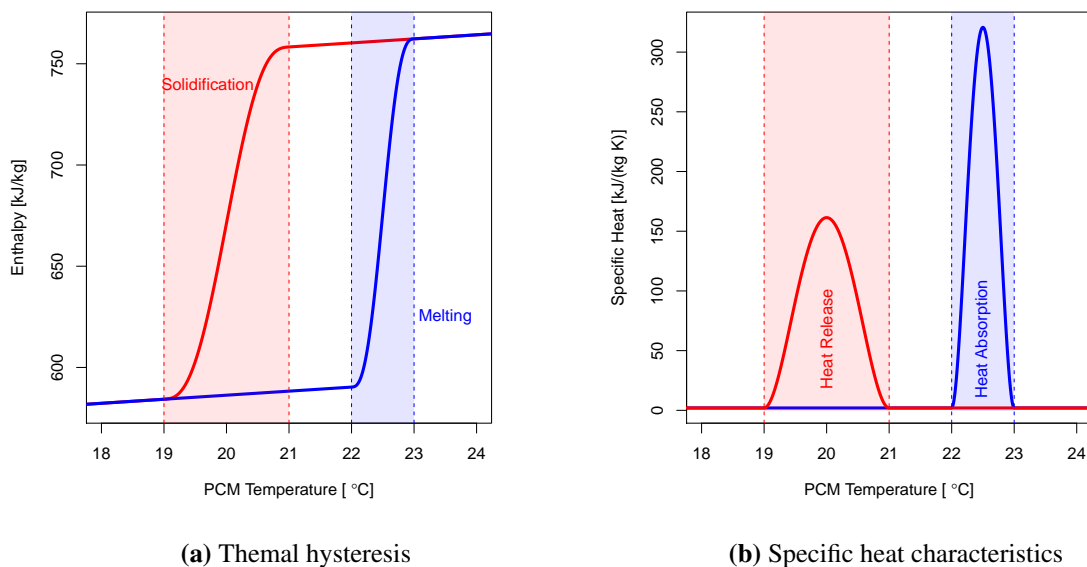
The current state of art in modeling phase change phenomena is based on the *apparent heat capacity method* which introduces an arbitrarily defined melting temperature range ΔT to smear out the rapidly changing thermal properties of the PCM in the freezing and melting cycle [4]. The detailed setup, analysis and discussion for a validated higher dimension test-case is thoroughly described by [2] while this physical model is restricted to the heat conduction case as sketched in Figure 1. The modeling tool considers 1D geometries. Figure 1 illustrates the setup for two exemplary wall constructions in Switzerland and Greece [5]. Here, the insulation layer thickness for the Swiss case is set to the minimum requirement to emphasize the benefit of PCM. To simulate the model one boundary condition at location ② is needed. There, a mixed Dirichlet-Neumann boundary condition is used for the ambient temperature and solar radiation. Domain interval ① represents a domain heat source to maintain the indoor temperature at human comfort level between 19°C and 26°C.

2.2. Thermophysical properties

Table 1 summarizes the thermophysical properties of the different layers involved in the wall structure [8]. The PCM is encapsulated in a mat intended for building purposes and comes with a freezing temperature of $19^{\circ}\text{C} < T_{freeze} < 21^{\circ}\text{C}$ while the melting occurs between $22^{\circ}\text{C} < T_{melt} < 23^{\circ}\text{C}$ [7]. In operation, a latent heat of 170 kJ kg^{-1} is released or absorbed. Due to the broad melting and freezing temperature ranges both phases may coexist depending on the direction of heat supply. The characteristic thermal hysteresis this material exhibits is drawn in Figure 2a. Conveniently, the user-defined melting and freezing temperature range ΔT required by the apparent heat capacity method can be set to $\Delta T_{freeze} = 2\text{K}$ and $\Delta T_{melt} = 1\text{K}$ which corresponds to the reality for this particular PCM. The difference in ΔT is noted also in the specific heat characteristics as per Figure 2b. The heat release is smeared out over a larger temperature interval leading to a lower peak. In practice, this means that the PCM tends to release heat slower and absorb faster.

Table 1. Thermophysical properties of the different layers

Layer	Density ρ [kg m ⁻³]	Heat Capacity C_p [J kg ⁻¹ K ⁻¹]	Thermal Conductivity λ [W m ⁻¹ K ⁻¹]
Air	1.225	1000	0.02
Plaster	1100	1000	0.57
PCM	1400-1500	2000	0.6
Brick Wall	920	1000	0.4
PIR Insulation [5]	36	1400	0.02
EPS Insulation [6]	15	1500	0.04

**Figure 2.** Thermal properties of the selected PCM [7]

2.3. Typical meteorological year

The simulation is carried out by taking into account the dry bulb temperature and solar radiation for Brugg-Windisch in Switzerland and Thessaloniki, Greece from October until December. The weather data is retrieved from the standardised *Typical Meteorological Year* (TMY). Figure 3 shows the data fed into boundary ②.

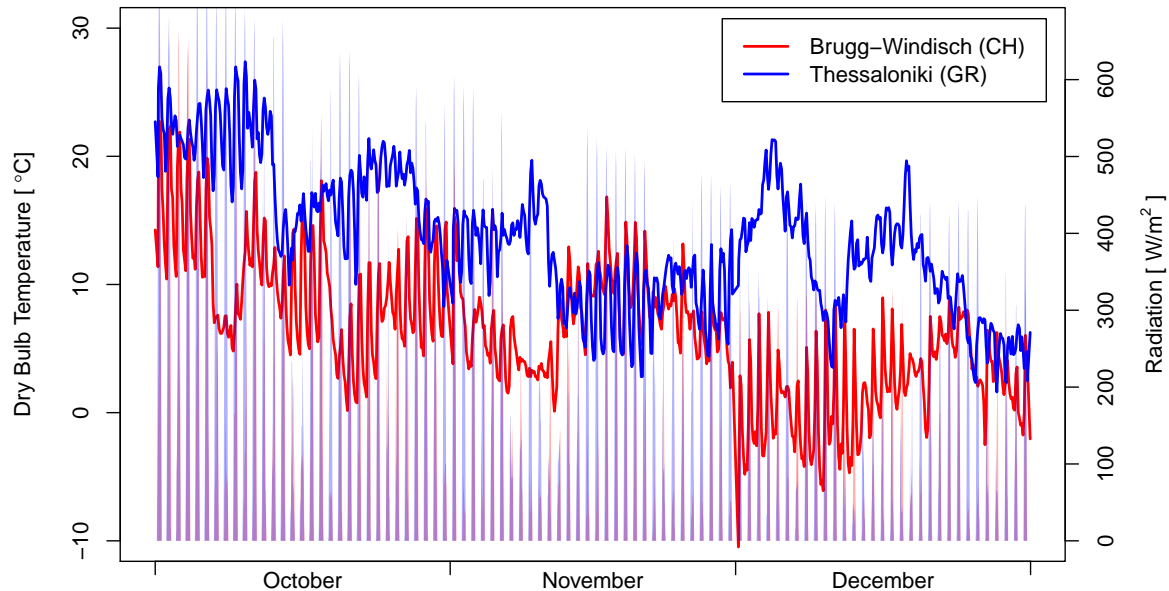


Figure 3. Typical meteorological year data for the selected locations Brugg-Windisch and Thessaloniki in Switzerland and Greece, respectively. Radiation values according to the same color scheme for Brugg-Windisch (red) and Thessaloniki (blue).

3. Numerical Model

The following modeling approach is specifically designed for the software tool COMSOL Multiphysics.

3.1. Pre-definition of parameters

Table 2 lists the recommended parameters in the *Global Parameters* section of the software. This best practice is particularly efficient for conducting parametric studies. Note that two new characteristic temperatures have been introduced, T_{top} and T_{bottom} , which represent the upper and lower limit of fully liquid state and fully solid state, respectively. With T_{bottom} being 19°C for the Rubitherm SP21EK the initial temperature T_0 is set arbitrarily to 16°C to ensure a fully solid state as starting point.

Table 2. Parameters for the simulation

Name	Expression	Description
L_plaster	50 [mm]	Length Plaster Layer
L_brick	175 [mm]	Length Brick Wall Layer
L_PCM	20 [mm]	Length PCM Layer
L_insul	80 [mm]	Length Swisspor PIR Top023 Layer
L_air	50 [mm]	Length Air Layer
dT_melt	1 [K]	PCM Melting Temperature Range
dT_freeze	2 [K]	PCM Freezing Temperature Range
Cp0	2 [kJ/(kg K)]	PCM Specific Heat Capacity
rho_l	1400 [kg/m ³]	PCM Liquid Density
rho_s	1500 [kg/m ³]	PCM Solid Density
LH	170 [kJ/kg]	PCM Latent Heat of Fusion
T_melt	22.5 [degC]	PCM Melting Temperature
T_freeze	20 [degC]	PCM Freezing Temperature
T_top	$T_{\text{melt}} + dT_{\text{melt}}/2$	PCM Fully Liquid Temperature
T_bottom	$T_{\text{freeze}} - dT_{\text{freeze}}/2$	PCM Fully Solid Temperature
k	0.6 [W/(m*K)]	PCM Thermal Conductivity
T0	16 [degC]	Initial Temperature of System

3.2. Geometry

To build the geometry select *Component 1* \rightarrow *1D* and include an *Interval* subnode. The definition of the different intervals for the layers of the wall crosssection follows this scheme

```

0
L_air
L_air + L_plaster
L_air + L_plaster + L_PCM
L_air + L_plaster + L_PCM + L_brick
...
```

which depicts the situation for the Swiss standard-setting the coordinates and creating subdomains for each layer according to Figure 1. With this systematic procedure in building the geometry, the layers can easily be exchanged to examine different locations [9]. In the case of the Greek building standard an additional parameter L_brick2 for the outer brick wall is required. The length of the air layer is chosen in a way that near-wall effects can be avoided. However, for a more complete and accurate calibration it is recommended to include convective phenomena.

3.3. User-defined functions

The pre-defined parameters and geometry pose the basis to implement the phase change functionality and import meteorological data. To achieve the correct implementation it is recommended to use the feature *User-defined functions* within the software. The following steps ensure a coherent representation of the rapid changes in thermophysical properties as the PCM turns solid or liquid [3, 10, 11].

- **Step Functions** Add a *Step1* function from the *Definitions* subnode ranging from 0 to 1 with a transition size range *dT_freeze*. Add an analogous step-function for the melting temperature. Use a second-derivative smoothing to avoid numerical singularities in the evaluation of the Heaviside Step Function.
- **Enthalpy Function** Add an analytic function with name *H_StoL* found under *Analytic* in the *Definitions* subnode. The expression is $Cp0*T+LH*step2(T-T_{melt}[1/K])$ with argument *T*. The unit for the argument is K and for the function J/kg. In the same way, a separate enthalpy function for the liquid to solid enthalpy *H_LtoS* is defined as $Cp0*T+LH*step1(T-T_{freeze}[1/K])$.
- **Specific Heat Function** Add an analytic function with name *Spec_StoL* found under *Analytic* in the *Definitions* subnode. The expression is the temperature derivative of the enthalpy function which can conveniently be defined in COMSOL with the derivative operator as $d(Cp0*T+LH*step2(T-T_{melt}[1/K]),T)$ with argument *T*. The unit for the argument is K and for the function J/(kg*K). The specific heat function for the liquid to solid process is defined analogously.
- **TMY** Choose *Interpolation* from the *Definitions* subnode to read in text file data for the typical meteorological year for the dry bulb temperature and radiation. It is recommended to retrieve data hourly. As such, set the argument unit to h and the function units to degC and W/m². The data shall be retrieved from external sources for the time interval of interest. In this case the variables are named *TMY_BruggWindisch_T* and *TMY_BruggWindisch_W* both being functions of time. Similarly for Thessaloniki.
- **Coupling - Average** With the intention of maintaining the indoor temperature at human comfort level an average variable for the first geometry interval *L_air* is defined. This is used to dynamically compute the average indoor temperature with every iteration and supply heat from an external source if the average indoor temperature falls below 19°C. To implement this functionality choose the operator *Average* from the *Definitions* subnode with the variable name *aveop1*. Select the first interval for the domain entity to be averaged. In a separate *Variables* node make the computed indoor temperature value available by defining $T_s = aveop1(T)$.

3.4. Materials

The simulation features different kinds of materials according to the listing in Table 1. It is recommended to type in the materials as listed in separate *Blank Material* subnodes and selecting the corresponding material intervals to define the exact position. The properties of air may be imported from the internal material library.

3.5. Heat transfer equation

The transient heat conduction in 1D is described by the following heat transfer equation

$$A_c \rho C_p \frac{\partial T}{\partial t} - \nabla \cdot (A_c k \nabla T) = q_0 \quad (1)$$

with A_c being the cross-sectional area of the 1D line as 1 m² by default, ρ being the material density, T the dependent variable for the temperature, t the time, k the thermal conductivity and q_0 any additional heat sources or sinks. In COMSOL this equation is found predefined under *Physics* → *Heat Transfer in Solids*.

With the assignment of materials to the specific domains as previously the tool recognizes automatically the thermodynamical couplings between the layers. The PCM layer, however, requires a separate definition. To achieve the correct implementation add a *Solid/Fluid* domain subnode and select the PCM layer. Under section *Thermodynamics, Solid* define the density as $SL * rho_l + (1-SL) * rho_s$ and the heat capacity as $SL * Spec_StoL(T) + (1-SL) * Spec_LtoS(T)$. This way it is ensured that the simulation takes the correct value for the solid or liquid phase. The

variable SL accounts for the direction of the heat transfer, from solid to liquid or *vice versa*, respectively. The dynamic computation of SL is described in the next subsection 3.6. Table 3 summarizes the boundary conditions used in the simulation.

Table 3. Boundary conditions to solve the heat transfer equation (1)

Boundary	Type	Remarks
①	Domain Source	Technically this is a domain condition to cover the external energy demand. Add a <i>Heat Source</i> node with heat rate $3[\text{W}]*\text{Thermostat}$. For a larger heater, increase the power input. The variable <i>Thermostat</i> is an integer 0 or 1, switching on and off the heat supply.
②	Dirichlet-Neumann	Mixed boundary condition for the dry bulb temperature and solar radiation. Add a <i>Temperature</i> node with value $\text{TMY_BruggWindisch_T}(t)$ and a <i>Heat Flux</i> node with value $\text{TMY_BruggWindisch_W}(t)$

3.6. Direction of heat transfer

Especially for PCM with thermal hysteresis behavior it is important that the solver knows the instantaneous phase state. To implement this, a new variable SL is introduced by an ordinary differential equation [10]. In COMSOL notation the *Domain ODE* proves a suitable candidate

$$e_a \frac{\partial^2 \text{SL}}{\partial t^2} + d_a \frac{\partial \text{SL}}{\partial t} = f \quad (2)$$

where the damping and mass coefficients, e_a and d_a , are set to zero. The variable SL is evaluated by the source term, which is defined with logical operators as

$$f = \text{SL} - \text{nojac}(\text{if}(\text{T} > \text{T}_{\text{top}}, 0, \text{if}(\text{T}_{\text{bot}}, 1, \text{SL}))).$$

The `nojac()` command ensures that the iteratively computed value of SL is merely evaluated at each time-step instead of being differentiated which may raise numerical instabilities. In practice, the SL variable acts as tracker for the current melted fraction and the initial value has to be chosen accordingly. For a fully solid state at $t = 0$ s the variable is 1, and 0 for the fully liquid state.

3.7. Thermostat functionality

To maintain the indoor temperature at human comfort level between 19 and 26°C another variable *Thermostat* is introduced which is implemented via the *Events* interface [11]. The benefit of using a temperature range instead of a fixed Dirichlet indoor temperature is to create a more realistic heat transfer process.

A priori the point in time where the heater turns on or off is not known. Therefore, an indicator state is necessary to tell the solver when heating supply is required. To do so, the events interface is customized according to Table 4.

Table 4. Definition of the *Events* interface to implement thermostat functionality

Node	Value	Remarks
Discrete States	1 / 0	The initial value is 1 if the heat is supplied from the beginning, <i>i.e.</i> $T < 19^{\circ}\text{C}$. Otherwise leave the initial value to 0.
Indicator States 1	Top = $T_s - 26$ [degC]	Iteratively compute the variable Top as an indicator for temperature surplus.
Indicator States 2	Low = $T_s - 19$ [degC]	Iteratively compute the variable Low as an indicator for temperature deficit.
Implicit Event 1	Top > 0	When the average value of the indoor temperature T_s reaches 26°C the value of Thermostat is set to 0.
Implicit Event 2	Low < 0	When the average value of the indoor temperature T_s falls below 19°C the value of Thermostat is set to 1.

3.8. Solver settings

The study is solving the heat transfer equation together with the additional ordinary differential equation for the phase state and the implicit logical condition variables for the thermostat functionality. These three components are solved simultaneously in a coupled manner. The transient study runs from $t = 0\text{s}$ to the final value of observed timespan. Here, the TMY months of October, November and December are considered which yields times of 0 to 2207 hours. In *Study Settings* set the value to `range(0, 1, 2207)` where 1 gives a writing results interval of 1 hour.

Further finetuning is achieved by modifying the default solver to a segregated solver found under *Time-Dependent Solver* \rightarrow *Segregated*. For the accurate tracking of the current phase, solid or liquid, include the phase state variable SL within the *Previous Solution* environment in the time-dependent solver settings.

On a desktop workstation with 16 CPUs and 32GB RAM each simulation run is completed within 15-20 seconds.

4. Results

4.1. Comparison between Switzerland and Greece

The presented modeling guideline is used to evaluate the PCM performance for the wall crosssections illustrated in Figure 1 fed with the TMY data for dry bulb temperature and solar radiation between October and December. The diagrams in Figure 4 compare the situation in Switzerland and Greece. The PCM performance over the observed time-span is characterized by the SL variable which indicates the current phase state.

Over the whole timespan the PCM layer in Switzerland according to Figure 4a remains solid meaning that heat is constantly released. The temperature curve starts from an initial value of 16°C until slightly above 22°C where the PCM temperature remains almost constant. The PCM never crosses the solid-to-liquid temperature of 23°C and therefore it can be assumed that heat is supplied by both PCM and heater to maintain the indoor temperature at a comfortable level. As the PCM supplies heat the phase change process is ongoing. The red curve in Figure 5 shows the required heat input for Switzerland which has a large peak and several oscillations at the beginning of October. Afterwards, the system stabilizes and no more external energy input is necessary.

The situation in Greece differs from the Swiss one as the PCM undergoes a phase change twice. The first one, from solid to liquid, at the beginning of November and the second one, from liquid to solid, towards the end of december. During the phase change the PCM suffers strong temperature variations. The heating and cooling demand in Figure 5 depicted by the blue curve for Thessaloniki shows that

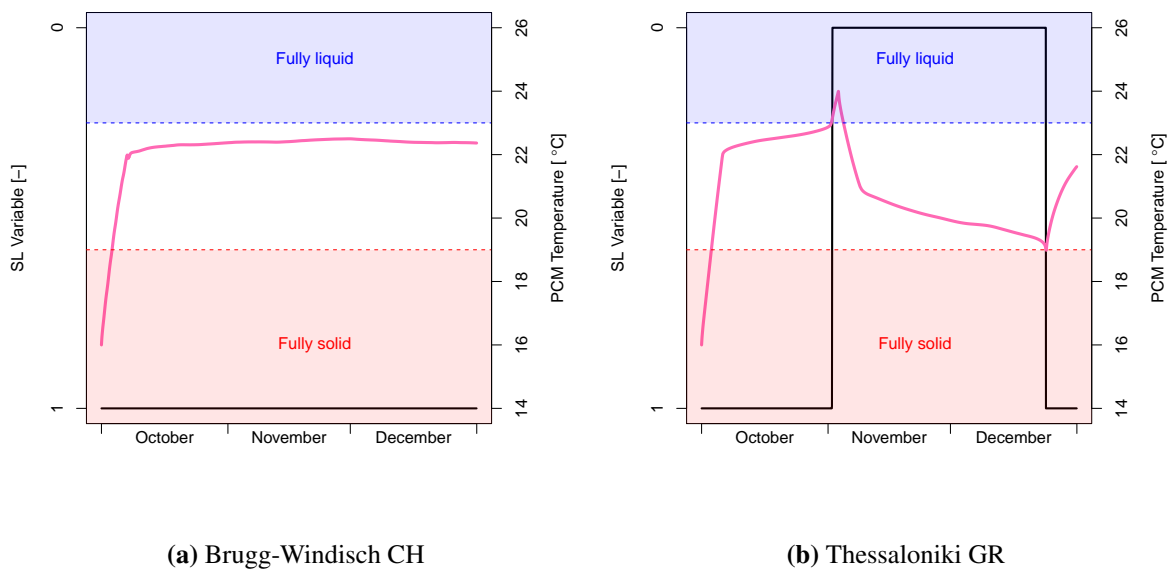


Figure 4. Comparison of the PCM performance by means of the dynamically computed SL variable as an indicator for solid or liquid state as well as the PCM temperature.

the system starts with indoor heating at the beginning of October. However, around the beginning of November there is an excess of heat that needs to be eliminated to maintain a comfortable indoor temperature. Here, the heat absorption due to phase change is not enough, and thus, the system requires additional energy input for air conditioning. Shortly after, the two large energy peaks in both directions appear. Towards the end of December the PCM undergoes another phase change from liquid to solid to supply heat which is assisted a little by an external heater.

4.2. Discussion

The results for the Swiss analysis show that the placement of a PCM mat in the layering of the wall crosssection might be beneficial to reduce energy costs [12, 13]. In fact, the indoor temperature can be kept at human comfort level with little energy input at the beginning of October. To quantify the thermal benefit a separate study without PCM according to the presented modeling scheme can be conducted. Interestingly, the simulation for the Greek environment shows several oscillations in both phase change and external energy input. This is evidence that the use of a PCM is only reasonable when considered within the extended dynamics of heat transfer processes. In fact, most datasheets characterize the PCM by its freezing temperature which is mistakenly equated to the indoor temperature. During the design process, it is of utmost importance to calibrate the PCM in the larger context of heat dynamics to ensure that it fulfills thermal requirements. A poorly placed PCM may result in an increase of cooling demand [9].

The SL variable pictured in Figure 4 accounts for the direction of the heat transfer which is crucial for PCM that exhibit thermal hysteresis. As such, the SL variable tells the solver which enthalpy curve to follow as per Figure 2a. However, the SL variable may not be confused with the melted fraction θ which indicates the amount of melted material. For a $\theta = 0$ the PCM is fully solid, while for a $\theta = 1$ the PCM is fully liquid. In order to calculate the melted fraction in a hysteresis PCM two distinct values, θ_s and θ_m , must be considered first. The general formula to obtain the fraction is

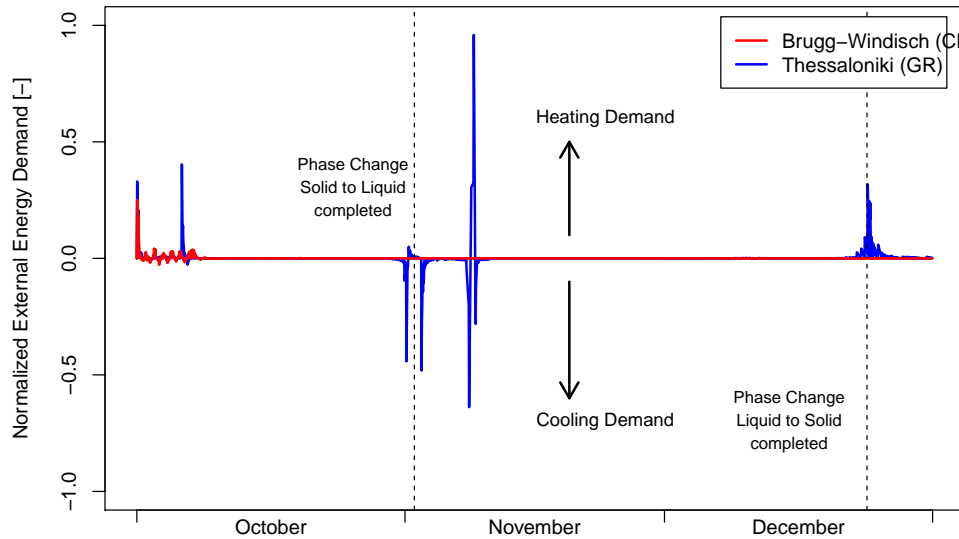


Figure 5. Thermal performance of the analysis. The energy demand is evaluated numerically by the source term variable and normalized by the peak value of energy demand.

$$\theta(T) = \begin{cases} 0, & \text{for } T < T_a - \Delta T/2 \\ \frac{T - (T_a - \Delta T/2)}{\Delta T}, & \text{for } T_a - \Delta T/2 < T < T_a + \Delta T/2 \\ 1, & \text{for } T > T_a + \Delta T/2. \end{cases} \quad (3)$$

where $\theta(T)$ is the instantaneous PCM temperature, T_a the arithmetic mean between freezing and melting temperature (here, $T_{a,s} = 20^\circ\text{C}$ and $T_{a,m} = 22.5^\circ\text{C}$) and ΔT the melting temperature range (here, $\Delta T_s = 2\text{ K}$ and $\Delta T_m = 1\text{ K}$). Note that the subscripts s and m refer to the two separate enthalpy curves (melting, solidification) according to Figure 2a. To obtain the instantaneous melted fraction, $\theta(T)$, with respect to the current heat transfer direction variable SL, the following relation holds

$$\theta(T, SL) = SL\theta_s(T) + (1 - SL)\theta_m(T) \quad (4)$$

In COMSOL the case-by-case analysis for the melted fraction is conveniently constructed by two nested if () operators with logicals as

$$\begin{aligned} \theta_s &= \text{if}(T < 19[\text{degC}], 0, \text{if}(T > 19[\text{degC}] \ \&\& \ T < 21[\text{degC}], (T - 19[\text{degC}])/2[\text{K}], 1)) \\ \theta_m &= \text{if}(T < 22[\text{degC}], 0, \text{if}(T > 22[\text{degC}] \ \&\& \ T < 23[\text{degC}], (T - 22[\text{degC}])/2[\text{K}], 1)). \end{aligned}$$

Figure 6 shows the application of the modeling methodology in this work for a full meteorological year according to the Greek setup. In this case, heat gains by solar radiation indoors is added by assuming an 1 m^2 window and a solar heat gain coefficient of 0.5 which is implemented in the model as an additional heat flux node on boundary (1). Apparently, the PCM chosen has a limited performance especially in the summer months where the PCM is fully liquid and cannot fully exploit its buffering capabilities. This example shows the need of assisting PCM-design and development in the built environment with numerical models. The presented model in this work is thermodynamically fully coupled and suitable to assess the thermal performance of a specific setup. To improve the thermal benefit in a PCM in this particular case the civil engineer may consider using a PCM with a more elevated melting temperature

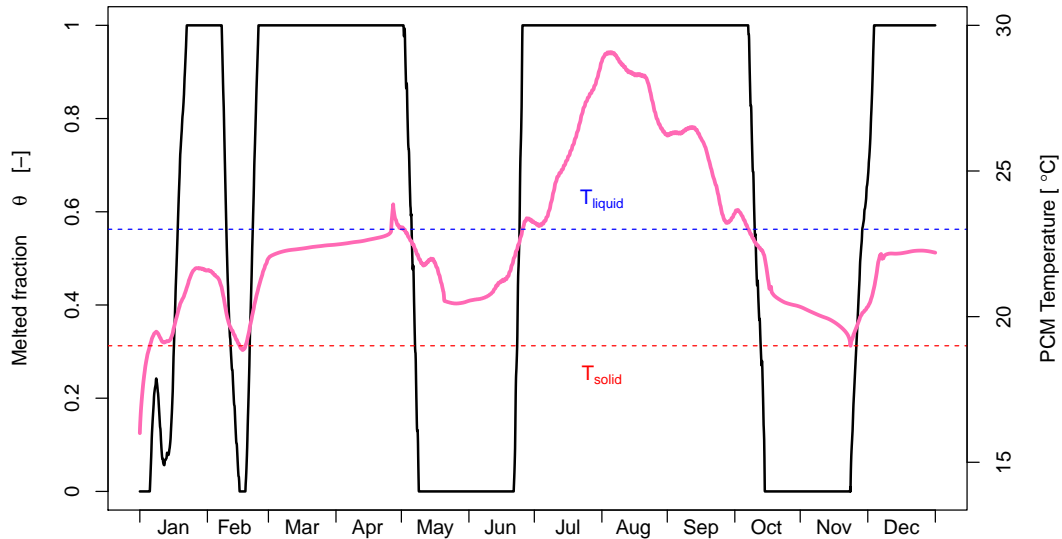


Figure 6. Melted fraction $\theta(T)$ over a full typical meteorological year for the Greek setup considered in this work. The black curve indicates the phase changes. $\theta(T) = 1$ means fully liquid and $\theta(T) = 0$ fully solid.

to smear out peak temperatures in summer, use a second layer on the outer surface of the wall or both combined.

5. Conclusion

The modeling guideline presented in this work aims at assisting the engineering of sustainable buildings by aid of phase change materials at an early development stage. It bridges the gap between material and room level analysis of PCM, thus, providing a suitable orientation tool in the selection of a material that fulfills technical, economic and thermal requirements. The 1D conduction approach proves convenient to qualitatively assess the performance of a specific PCM submitted to indoor heating and cooling in combination with meteorological data. Further extension of the modeling framework may include near-wall effects and indoor solar radiation dynamics. In this work, the latter is present only in the Greek year-round showcase. Such adjustments require the sole modification of energy supply by the boundary conditions.

References

- [1] Agyenim F, Hewitt N, Eames, P and Smyth M 2010 A review of materials, heat transfer and phase change problem formulation for latent heat thermal energy storage systems (LHES). *Renew Sust Energ Rev.* **14** 615-628. DOI: 10.1016/j.rser.2009.10.015
- [2] Rubinetti D, Weiss D A, Chaudhuri A and Kraniotis D 2018 Convective melting modeling approach for phase change materials with variable boundary heating *59th Scandinavian Conf. on Simulation and Modeling (Oslo)* **153** 103-110. DOI:10.3384/ecp18153103
- [3] Rubinetti D, Weiss D A, Chaudhuri A and Kraniotis D 2018 Modeling approach to facilitate thermal energy management in buildings with phase change materials *COMSOL Conference 2018 (Lausanne)*.
- [4] Al-Saadi S N and Zhai Z 2015 Systematic evaluation of mathematical methods and numerical schemes for modeling PCM-enhanced building enclosure *Energy Build.* **92** 374-388. DOI: 10.1016/j.enbuild.2015.01.044
- [5] Swisspor AG 2018 Aussenwaende. <https://www.swisspor.ch/index.php?section=datasheet&cmd=planningPage&id=5822>
- [6] Sagex AG 2015 EPS insulation materials. <https://www.sager.ch/en-gb/products-and-prices/catalogs/sagex-product-catalog.pdf>
- [7] Rubitherm Technologies GmbH 2016 Technisches Datenblatt SP21EK. https://www.rubitherm.eu/media/products/datasheets/Techdata_-SP21EK_DE_30092016.PDF
- [8] Izquierdo-Barrientos M A, Belmonte J F, Rodriguez-Sanchez D, Molina A E and Almendros-Ibanez J A 2012 A numerical study of external building walls containing phase change materials (PCM) *Appl Therm Eng.* **47** 73-85. DOI: 10.1016/j.applthermaleng.2012.02.038
- [9] Xing J, Medina M. A. and Zhang Xiaosong 2016 Numerical analysis for the optimal location of a thin PCM layer in frame walls *Appl Therm Eng.* **103** 1057-1063. DOI: 10.1016/j.applthermaleng.2016.04.056
- [10] Frei W 2016 Thermal modeling of phase-change materials with hysteresis. URL: www.comsol.com/blogs/thermal-modeling-of-phase-change-materials-with-hysteresis
- [11] Frei W 2015 Implementing a thermostat with the events interface. URL: www.comsol.com/blogs/implementing-a-thermostat-with-the-events-interface
- [12] Srinivasan PSS and Ravikumar M 2014 Heat transfer analysis in PCM-filled RCC roof for thermal management *J. Mech. Sci.* **28** 1073-1078. DOI: 10.1007/s12206-013-1137-0
- [13] Fleischer A S 2015 *Thermal energy storage using phase change materials: fundamental and applications* (Cham: Springer International Publishing)